(1990); V. Tvergaard and J. W. Hutchinson, *J. Am. Ceram. Soc.* **71**, 157 (1988)] allow one to estimate properties of the microscopic deviatoric stress for particular material properties. These studies reveal that the microscopic stress varies within individual grains, but the grain size should not affect the amplitude of the microscopic stress field [A. G. Evans and D. R. Clarke, in *Thermal Stresses in Severe Environments*, D. P. H. Hasselman and R. A. Heller, Eds. (Plenum, New York, 1980), pp. 629–649].
14. M. H. Grimstitch and A. K. Ramdas, *Phys. Rev. B* **11**, 3139 (1975).
15. T. N. Loladze and G. V. Bockuchava, in *New Developments in Grinding*, First Proceeding of the International Grinding Conference (Carnegie Press, Pittsburgh, PA, 1972), pp. 432–448.
16. B. Evans and C. Goetze, *J. Geophys. Res.* **84**, 5505 (1979).
17. T. Evans and M. Omar, *Philos. Mag.* **7**, 843 (1953).
18. See, for example, H. J. Frost and M. F. Ashby, *Deformation-Mechanism Map: The Plasticity and Creep of Metals and Ceramics* (Pergamon, New York, 1982), p. 166.
19. R. C. DeVries, *Mater. Res. Bull.* **10**, 1193 (1975).
20. M. Schrauder and O. Nevon, *Nature* **365**, 42 (1993).
21. B. H. Scott-Smith, R. V. Danchin, J. W. Harris, K. J. Stracke, in *Kimberlites I: Kimberlites and Related Rocks*, vol. 11A of *Developments in Petrology*, J. Kornprobst, Ed. (Elsevier, Amsterdam, 1984), pp. 121–142. Also see S. E. Kessen and J. D. Fitz Gerald, *Earth Planet. Sci. Lett.* **111**, 229 (1991).
22. Supported by National Science Foundation grant EAR9219245.

31 May 1994; accepted 24 August 1994

Vibrationally Coherent Photochemistry in the Femtosecond Primary Event of Vision

Qing Wang, Robert W. Schoenlein, Linda A. Peteanu,* Richard A. Mathies, Charles V. Shank

Femtosecond pump-probe experiments reveal the impulsive production of photoproduct in the primary event in vision. The retinal chromophore of rhodopsin was excited with a 35-femtosecond pulse at 500 nanometers, and transient changes in absorption were measured with 10-femtosecond probe pulses. At probe wavelengths within the photoproduct absorption band, oscillatory features with a period of 550 femtoseconds (60 wavenumbers) were observed whose phase and amplitude demonstrate that they are the result of nonstationary vibrational motion in the ground state of the photoproduct. The observation of coherent vibrational motion of the photoproduct supports the idea that the primary step in vision is a vibrationally coherent process and that the high quantum yield of the cis→trans isomerization in rhodopsin is a consequence of the extreme speed of the excited-state torsional motion.

The first step in vision, the light-induced isomerization of the retinal chromophore in rhodopsin, is complete in only 200 fs, making it one of the fastest photochemical reactions (*1*–*3*). Our previous studies suggested that coherent nuclear motion might accompany this ultrafast, highly efficient (quantum yield = 0.67) reaction because the 200-fs reaction time is comparable to or less than the period of torsional vibrations of the retinal chromophore (*4*). Does vibrational coherence play an important role in the first step in vision? Femtosecond optical techniques provide a powerful tool for examining the role of vibrational coherence in ultrafast reactions by creating coherent states of matter that reflect the motion of individual molecules. We report the observation of coherent vibrational motion in the photoproduct of the ultrafast isomerization in rhodopsin. Our results indicate that the isomerization proceeds along a diabatic pathway connecting the excited state of the 11-cis reactant with the ground state of the all-trans photoproduct (Fig. 1). The coherent nuclear dynamics observed here reveal the intimate connection between the speed of the cis→trans isomerization in rhodopsin and its photochemical quantum yield, thereby establishing a new paradigm for the photochemistry of vision.

Vibrational coherence is a natural consequence of nonstationary vibrational states excited by femtosecond optical pulses [see (*5*)] and can result from at least three elementary processes (*6*). First, coherent vibrational motion of the reactant in the ground state can be produced by femtosecond excitation through stimulated Raman scattering. For example, nonstationary ground-state vibrational motion has been observed in molecular crystals (*7*) and in the biological pigment bacteriorhodopsin (*6*, *8*). Second, vibrational coherence can be produced on the excited-state potential energy surface and has been observed in a variety of dye molecules in solution (*9*), in small molecules in the gas phase (*10*, *11*), and in bacteriorhodopsin (*12*). Recently, excited-state vibrational coherence has also been observed in photosynthetic reaction centers (*13*). The third case is where vibrational coherence persists throughout the time course of a photochemical reaction and is observed in the product. This case is the most interesting because it elucidates the role of nonstationary states in the ultrafast reaction dynamics. Such coherence has been observed in the ultrafast photodissociation of I_3^- (*14*). We show here that coherent nuclear vibrations can also be observed in the product of an ultrafast photochemical reaction that occurs within a protein at room temperature.

Rhodopsin samples were prepared from bovine retinas and dissolved in Ammonyx LO detergent solution as described previously (*1*). Femtosecond pump-probe measurements were performed with 35-fs pump pulses at 500 nm, and transient changes in absorption were measured from 450 to 570 nm with 10-fs blue probe pulses and from 560 to 640 nm with 10-fs red probe pulses. The method for generating 35-fs pump pulses at 500 nm as well as 10-fs probe pulses is described elsewhere (*15*). The experimental configuration used to obtain time-resolved differential transmission spectra was identical to that used in previous experiments. The average pump power was ~3 μW at a repetition rate of 540 Hz. The pump (~0.5 mJ/cm^2) and probe (~0.04 mJ/cm^2) beams were focused in a 0.3-mm jet of flowing bovine rhodopsin (15 OD/cm). The flow rate was

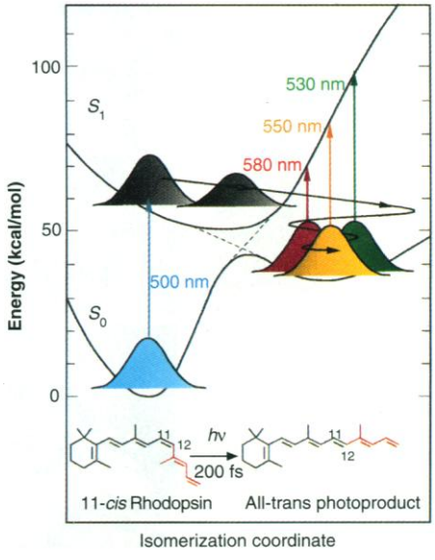

Fig. 1. Schematic potential energy surfaces for the femtosecond isomerization of rhodopsin after optical excitation of the molecule from the ground state S_0 to the excited state S_1. The wave packets in the photoproduct potential well illustrate how ground-state vibrational motion effects the photoproduct absorption. The dashed lines indicate the diabatic pathway along which the reaction proceeds.

Q. Wang and C. V. Shank, Materials Sciences Division, Lawrence Berkeley Laboratory, and Department of Chemistry, University of California, Berkeley, CA 94720, USA.
R. W. Schoenlein, Materials Sciences Division, Lawrence Berkeley Laboratory, Berkeley, CA 94720, USA.
L. A. Peteanu and R. A. Mathies, Department of Chemistry, University of California, Berkeley, CA 94720, USA.
*Present address: Department of Chemistry, Carnegie Mellon University, Pittsburgh, PA 15213, USA.

sufficient to replace the photolysed sample between successive pump pulses. Kinetic information at specific wavelengths was obtained by filtering the probe pulse after the sample (~7-nm bandpass) and combining differential detection with lock-in amplification as the pump-probe delay time was continuously varied. The differential transmittance signal ($\Delta T/T$) was a few percent or less and varied linearly with pump power.

Figure 2 presents differential transmission measurements probing within the photoproduct absorption band (maximum wavelength $\lambda_{max} \approx 550$ nm) after the excitation of 11-*cis* rhodopsin ($\lambda_{max} \approx 500$ nm) with a 35-fs pulse at 500 nm. All of these measurements exhibit the prompt appearance of photoproduct absorption within 200 fs, as observed previously (*1*, *2*). After the initial formation of photoproduct, we observe oscillatory features that have a period of ~550 fs in all the measurements. The fact that we are probing within the photoproduct absorption band suggests that these oscillations are due to ground-state photoproduct. However, it is important to develop an unambiguous test of this hypothesis because a number of processes can give rise to such vibrational coherences (6).

The spectral dependence of the oscillations provides critical information about their molecular origin. Figure 1 illustrates the behavior of a vibrationally coherent population with an absorption maximum near 550 nm corresponding to the photoproduct. The vibrational motion is depicted by the oscillation of a nonstationary wave packet in the potential well of the all-trans photoproduct. This harmonic motion results in a particularly strong modulation of the photoproduct absorption where the slope of the absorption is largest (~530 and ~580 nm) and a weaker modulation in the wings and near the peak of the absorption band (~550 nm). Furthermore, the modulation on the red side of the absorption maximum is out of phase with the modulation on the blue side of the absorption maximum. A vibrationally coherent population in the reactant ground state exhibits similar oscillatory behavior but the 180° phase shift occurs about the 11-*cis* rhodopsin absorption maximum of 500 nm instead of 550 nm. Such ground-state oscillations have been analyzed in detail in the case of bacteriorhodopsin (6). Thus, the origin of the vibrational coherence can be determined by analyzing the phase and amplitude of the oscillations at different probe wavelengths. The oscillations seen here are unlikely to be due to the excited-state population because the fluorescence quantum yield of rhodopsin is only $\sim 10^{-5}$ and the excited-state lifetime is <100 fs (*16*).

By probing the reaction over a broader spectral range, we are able to assign the origin of the oscillations (Fig. 3A). Measurements near 500 nm indicate the bleaching ($\Delta T/T > 0$) of the ground-state reactant, whereas measurements near the photoproduct absorption maximum at 550 nm ($\Delta T/T < 0$) indicate the formation of photoproduct within 200 fs. Measurements at 500, 530, 580, and 610 nm all exhibit vibrational coherence with a period of ~550 fs, which persists for several picoseconds. The oscillatory feature at 550 nm contains higher frequency components.

An analysis of the frequency content of the oscillatory part of the detected response at each of the wavelengths is presented in the Fourier power spectra in Fig. 3B. A feature is observed at ~60 cm^{-1} (550-fs period) at all probe wavelengths. In addition, the amplitude of the ~60-cm^{-1} oscillation is small at probe wavelengths in the edges of the photoproduct absorption (500 and 610 nm), and the oscillations are largest at probe wavelengths on the steep sides of the absorption band (530 and 580 nm). Furthermore, at the photoproduct absorption maximum (550 nm), the ~60-cm^{-1} oscillation is diminished, and there is evidence of higher frequency oscillations.

The phases of the oscillations exhibit a strong wavelength dependence (Fig. 4), with the oscillations in the blue (500 and 530 nm) being out of phase with the oscillations in the red (580 and 610 nm). The 180° phase change occurs near 550 nm, the photoproduct absorption maximum. The phase and amplitude analysis provide compelling evidence that the oscillations that we are seeing are due to the vibrational coherence of the ground-state photoproduct and are not due to photophysical oscillations in the reactant ground state or in the excited state.

The 60-cm^{-1} oscillations most likely originate from a skeletal torsional mode of the chromophore that is associated with the isomerization reaction. It is perhaps not surprising that coherent nuclear motion is maintained through the reaction because the half-time of the photoproduct formation (~100 fs) is roughly a quarter of the vibrational period of a 60-cm^{-1} mode. This is consistent with the continuous motion of a nonstationary wave packet along the diabatic surface connecting the reactant and the photoproduct (Fig. 1) (*17*). The vibrational coherence of this 60-cm^{-1} oscillation persists for 1 to 2 ps, which is the time scale for conformational relaxation and vi-

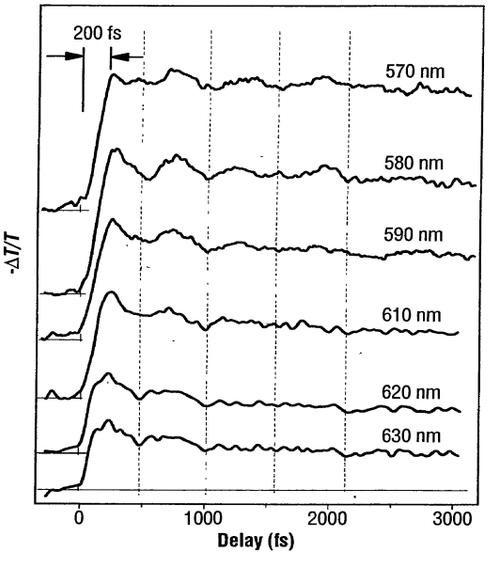

Fig. 2. Differential transient absorption measurements probing the photoproduct absorption after excitation of rhodopsin with a 35-fs pump pulse at 500 nm. Measurements at 620 and 630 nm are multiplied by a factor of 2 for clarity.

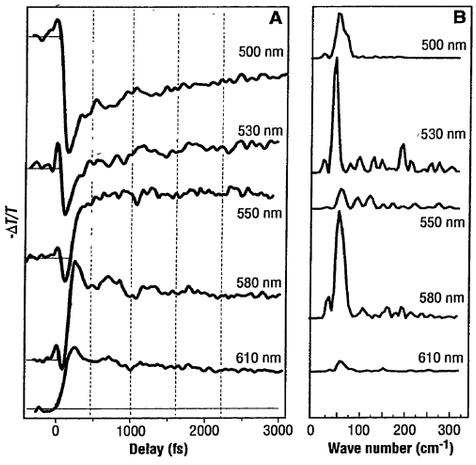

Fig. 3. (**A**) Differential transient absorption measurements probing a broad spectral range of the photoproduct absorption after excitation of rhodopsin with a 35-fs pump pulse at 500 nm. (**B**) Fourier transform analysis of the oscillations in the time-resolved data in (A). Before Fourier analysis, a smooth background consisting of a low-order polynomial fit was subtracted. The data at all wavelengths are transformed over the same time range of 200 to 3000 fs, with the lower limit constrained by the formation time of the photoproduct.

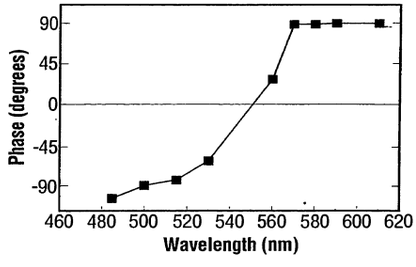

Fig. 4. Phase information derived from Fourier analysis of the oscillatory features in the data of Fig. 3. The relative phase of the oscillation is obtained by averaging the angular part of the Fourier transform from 50 to 70 cm^{-1}. For reference, the phase of the oscillations at 590 nm is set to ±90°.

brational cooling of the photoproduct (*2*). In addition, the high speed and quantum efficiency of the reaction require that the optical excitation couple strongly to the reactive mode(s) of the system, and that most of this energy remain localized along the reaction coordinate. Thus, the observation of 60-cm^{-1} oscillations after the isomerization strongly suggest that this vibrationally coherent mode has a large projection along the reaction coordinate. The oscillations reflect the torsional ringing of the all-trans chromophore around its equilibrium position after the rapid light-induced structural change.

The unprecedented speed of the isomerization process in rhodopsin coupled with the observation of coherent nuclear motion in the photoproduct suggests that the torsional motion of the chromophore is not significantly constrained by the protein environment. The chromophore appears to move relatively freely during the isomerization because the motion is relatively small and because the structure of the chromophore binding pocket accommodates the change in the chromophore structure (Fig. 5). This conclusion is consistent with an isomerization that occurs in the center of the chromophore with little motion at the ends (*18*). Resonance Raman studies (*19*) indicate that the overall structural change associated with the isomerization is relatively small because the 11-cis chromophore is already twisted along the reaction coordinate by the steric interaction between the C-13–CH_3 and the C-10–H groups and because the photoproduct does not immediately relax to a fully planar trans structure. Furthermore, the strong steric interaction between the C-13–CH_3 and the C-10–H likely aids the reaction process by providing a torsional force to the chromophore that rapidly drives it out of the Franck-Condon region after optical excitation (*3*, *20*).

The fact that vibrational coherence is maintained in the photoproduct of rhodopsin has important implications for the mechanism of the primary step in vision. In the traditional picture of this photochemical reaction, vibrational relaxation occurs rapidly on the excited-state potential energy surface (*21*). Internal conversion then proceeds from these thermalized vibrational states, with the excited-state→ground-state transition probability determined by the Fermi Golden Rule. However, our observation of vibrational coherence in the photoproduct strongly argues that the chromophore is not relaxed on the excited-state potential energy surface, nor is it critically damped along the reaction coordinate. Our results indicate that the 11-cis→all-trans reaction occurs in an essentially barrierless transition following a diabatic potential surface (indicated by the dashed lines in Fig. 1) (*1*). This surface carries the nonstationary wave packet rapidly and directly from the excited state of the reactant to the ground state of the product. Such nonstationary vibrational dynamics can be described as a Landau-Zener tunneling process, which expresses the quantum yield of a reaction P_{LZ} (probability of following the diabatic surface) in terms of the nuclear velocity v along the reaction coordinate as $P_{LZ} \propto \exp(-1/v)$ (*22–24*). Thus, if the nuclear dynamics along the isomerization coordinate are retarded, the quantum yield should be reduced (*25*). Indeed, femtosecond experiments on isorhodopsin, which has a slower isomerization speed (~600 fs) (*3*) and a correspondingly lower quantum yield (0.22), support this model. In conclusion, femtosecond spectroscopy has revealed the direct connection between nonstationary nuclear dynamics and the mechanism and quantum yield of the cis→trans isomerization in rhodopsin, thereby establishing a new paradigm for the photochemistry of vision.

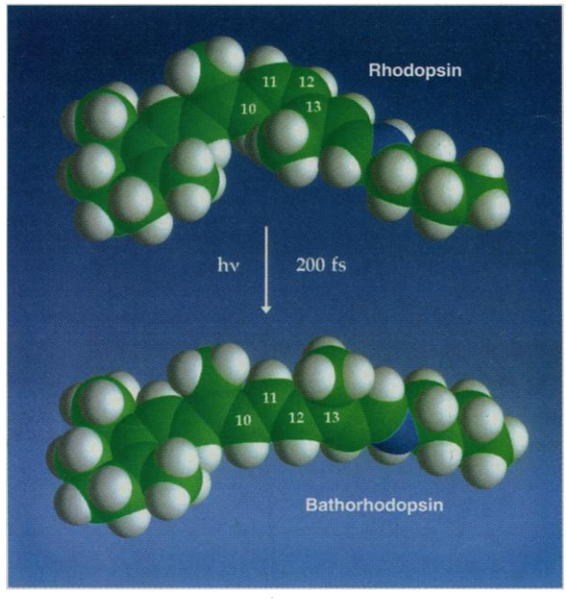

Fig. 5. Chromophore structural change in the first step of vision. The isomerization occurs in only 200 fs in part because the overall structural change is surprisingly small. The 11-cis reactant is twisted about the reaction coordinate because of the steric interaction between the C-13–CH_3 and C-10–H groups. In addition, the initial photoproduct is conformationally distorted such that the overall shape change required to achieve the C-11=C-12 isomerization is small (*19*).

REFERENCES AND NOTES

1. R. W. Schoenlein, L. A. Peteanu, R. A. Mathies, C. V. Shank, *Science* **254**, 412 (1991).
2. L. A. Peteanu, R. W. Schoenlein, Q. Wang, R. A. Mathies, C. V. Shank, *Proc. Natl. Acad. Sci. U.S.A.* **90**, 11762 (1993).
3. R. W. Schoenlein, L. A. Peteanu, Q. Wang, R. A. Mathies, C. V. Shank, *J. Phys. Chem.* **97**, 12087 (1993).
4. G. R. Loppnow and R. A. Mathies, *Biophys. J.* **54**, 35 (1988).
5. Vibrational coherence refers to a collective coherence among an ensemble of molecules and is a consequence of optical excitation on a time scale faster than the motion of interest. A short optical pulse also excites a manifold of quantized vibrational levels in a single molecule. These vibrational levels are coherent because they have specific phase and amplitude relations and therefore constitute a nonstationary vibrational state or wave packet that describes the nuclear motion. The vibrational coherence resulting from impulsive excitation reflects the nonstationary wave packet dynamics of individual molecules. Under continuous-wave excitation, vibrational coherence is not initiated in the ensemble. Nevertheless, the nonstationary wave packet dynamics of individual rhodopsin molecules are identical to that indicated by the femtosecond experiments.
6. W. T. Pollard *et al.*, *J. Phys. Chem.* **96**, 6147 (1992).
7. T. P. Dougherty *et al.*, *Science* **258**, 770 (1992).
8. S. L. Dexheimer *et al.*, *Chem. Phys. Lett.* **188**, 61 (1992).
9. H. L. Fragnito, J.-Y. Bigot, P. C. Becker, C. V. Shank, *ibid.* **160**, 101 (1989).
10. A. H. Zewail, *Science* **242**, 1645 (1988).
11. ———, *J. Phys. Chem.* **97**, 12427 (1993).
12. R. A. Mathies, C. H. Brito Cruz, W. T. Pollard, C. V. Shank, *Science* **240**, 777 (1988).
13. M. H. Vos, F. Rappaport, J.-C. Lambry, J. Breton, J. L. Martin, *Nature* **363**, 320 (1993).
14. U. Banin and S. Ruhman, *J. Chem. Phys.* **98**, 4391 (1993).
15. R. W. Schoenlein, J. Bigot, M. T. Portella, C. V. Shank, *Appl. Phys. Lett.* **58**, 801 (1991).
16. G. Kochendoerfer and R. A. Mathies, in *Proceedings of the Physical Chemistry Division, 208th National American Chemical Society Meeting*, Washington, DC (1994), abstr. 354.
17. A similar picture has emerged to describe the rapid photoisomerization of *cis*-stilbene [R. J. Sension, S. T. Repinec, A. Z. Szarka, R. M. Hochstrasser, *J. Chem. Phys.* **98**, 6291 (1993)].
18. A. Warshel, *Nature* **260**, 679 (1976).
19. I. Palings *et al.*, *Biochemistry* **26**, 2544 (1987).
20. A. Warshel and N. Barboy, *J. Am. Chem. Soc.* **104**, 1469 (1982).
21. T. Rosenfeld, B. Honig, M. Ottolenghi, J. Hurley, T. G. Ebrey, *Pure Appl. Chem.* **49**, 341 (1977).
22. B. Bagchi and G. R. Fleming, *J. Phys. Chem.* **94**, 9 (1990).
23. L. D. Landau, *Phys. Z. Sowjetunion* **2**, 46 (1932).
24. C. Zener, *Proc. R. Soc. London A* **137**, 696 (1932).
25. R. M. Weiss and A. Warshel, *J. Am. Chem. Soc.* **101**, 6131 (1979).

26. We thank Continuum Corporation for loaning us the MACH 500 YAG laser used for some of this work and S. J. Rosenthal for helpful discussions. This research was supported by Department of Energy contract DE-AC03-76SF00098 (C.V.S.), National Institutes of Health grant EY-02051 (R.A.M.), and National Science Foundation grant CHE 91-20254 (R.A.M.).

20 June 1994; accepted 24 August 1994